Preclinical Evaluation of the Penciclovir Analog 9-(4-[^{18}F]Fluoro-3-Hydroxymethylbutyl)Guanine for In Vivo Measurement of Suicide Gene Expression with PET

Mian M. Alauddin, Antranik Shahinian, Erlinda M. Gordon, James R. Bading, and Peter S. Conti

Department of Radiology, PET Imaging Science Center, University of Southern California, Los Angeles; and Gene Therapy Laboratory, Norris Comprehensive Cancer Center, University of Southern California, Los Angeles, California

The gene for herpes simplex virus thymidine kinase (HSV-tk) is widely used as a suicide gene in experimental gene therapy of cancer. 9-(4-Fluoro-3-hydroxymethylbutyl)guanine (FHBG) is an antiviral nucleoside analog that is rapidly phosphorylated by viral thymidine kinase but is a poor substrate for mammalian thymidine kinase. Recently, FHBG labeled in the 4-fluoro position with ^{18}F has shown promise relative to other similar compounds for imaging in vivo expression of HSV-tk using PET. In this study, we evaluated the uptake of [^{18}F]FHBG in vitro and in vivo using transduced and wild-type human colon cancer cells (HT-29). We also imaged [^{18}F]FHBG and measured the radioactivity concentrations of circulating [^{18}F]FHBG and its metabolites in monkeys. **Methods:** Sterile, pyrogen-free [^{18}F]FHBG was produced routinely in good yields. Cells were transduced with the retroviral vector G1Tk1SvNa containing HSV-tk gene. In vitro uptake studies were performed by incubating cells with [^{18}F]-FHBG at 37°C for 1 and 5 h. Biodistribution studies were performed at 2 and 5 h after injection in nude mice bearing tumors grown from wild-type or transduced cells. Sequential, whole-body PET scans of cynomolgus monkeys were obtained over a period of >2 h after intravenous injection of [^{18}F]FHBG. Arterial plasma samples obtained from monkeys 15–120 min after intravenous injection were subjected to acid extraction, and the acid-soluble fractions were analyzed by high-performance liquid chromatography. **Results:** In vitro studies showed 31 and 71 ($P < 0.001$) times higher uptake of the probe at 1 and 5 h, respectively, in transduced cells compared with nontransduced cells. In vivo studies in mice showed that tumor uptake of the radiotracer was 4-fold ($P < 0.05$) and 13-fold ($P < 0.001$) higher at 2 and 5 h, respectively, in tumors grown from transduced cells compared with control cells. Transduced tumor-to-normal tissue ratios ranged from 2 to 25 at 2 h and from 2 to 22 at 5 h. Recirculating labeled metabolites had only a minor effect on the biodistribution of radiolabel from [^{18}F]FHBG in monkeys. **Conclusion:** These results indicate that [^{18}F]FHBG may yield high-contrast PET images of HSV-tk expression in tumors and, therefore, it is a very promising radiotracer for monitoring of gene therapy of cancer with PET.

Received Feb. 8, 2001; revision accepted Jul. 12, 2001.

For correspondence or reprints contact: Peter S. Conti, MD, PhD, PET Imaging Science Center, University of Southern California, 2250 Alcazar St., Suite 101, Los Angeles, CA 90033-4609.

Key Words: PET; gene therapy; [^{18}F]FHBG; virus; colon cancer

J Nucl Med 2001; 42:1682–1690

Many antiviral nucleoside analogs are known to localize selectively in herpes simplex virus (HSV)-infected cells because of monophosphorylation catalyzed by virus-encoded thymidine kinase (*1–6*). Among these, acyclovir, ganciclovir, and penciclovir are reported to be potent against HSV types 1 and 2 (*7–12*). A viral thymidine kinase of low substrate specificity converts the nucleoside analogs to monophosphates (*2,4,6*), which are converted to diphosphates and then to the corresponding triphosphates by cellular enzymes, leading to inhibition of DNA polymerase (*9*).

The selective monophosphorylation of antiviral nucleoside analogs by virus-encoded thymidine kinase has been exploited in gene therapy of cancer (*13–15*). Gene therapy for treatment of human disease is currently being explored, and several approaches have been tested in patients (*16*). In this process, murine cells that are engineered to produce retroviral vectors that carry the gene for HSV thymidine kinase (HSV-tk) are injected into a tumor. Drug sensitivity is conferred upon tumor cells after expression of the HSV-tk gene. Ganciclovir is converted by the resulting HSV-tk to the monophosphorylated product, which is then converted to di- and triphosphates by host kinases, leading to tumor cell death (*15*). This approach is effective in the treatment of experimental glioma (*13,15*), hepatoma (*17*), and melanoma (*18*).

Treatment planning and individualization of gene therapy could be aided by a noninvasive method for measuring monophosphorylation induced in tumors to assess whether a therapeutically sufficient enzyme level exists before application of the prodrug ganciclovir (*19,20*). Moreover, the measurement of therapy effects on tumor metabolism of nucleoside analogs may be useful for predicting therapeutic outcome at an early stage of treatment (*21*).

PET using tracers of tumor metabolism has been used in the diagnosis and evaluation of treatment response in a variety of tumors (*22*). Development of PET for monitoring gene therapy with the suicide gene HSV-tk is underway (*19–21,23–31*). Many of these studies are designed to use a fluoro analog of ganciclovir, 9-([3-fluoro-1-hydroxy-2-propoxy]methyl)guanine (FHPG) (*24,25,27–31*). FHPG is selectively phosphorylated by HSV-tk at two thirds the rate of thymidine (*9*). Absence of viral kinase in noninfected cells precludes phosphorylation and, hence, trapping within these cells. [^{18}F]FHPG has been shown to be potentially useful as a PET imaging agent of gene expression and incorporation in transduced tumors (*24,27–31*).

Penciclovir, a carba analog of ganciclovir, is active against HSV types 1 and 2, varicella-zoster virus, and Epstein–Barr virus (*8,12*). Preliminary work from our group showed that the fluoro analog of penciclovir, 9-(4-fluoro-3-hydroxymethylbutyl)guanine (FHBG), is selectively phosphorylated by HSV-tk and has higher accumulation in transduced cells than does FHPG (*26*). This finding suggests that [^{18}F]FHBG might be better than [^{18}F]FHPG in PET imaging of gene expression in tumors. Recently, [^{18}F]FHBG has shown considerable promise relative to other indicators of HSV-tk expression in preliminary imaging studies in small animals (*32–35*). In this study, we report a detailed evaluation of this tracer in cell culture and in tumor-bearing nude mice using transduced and nontransduced HT-29 human colon cancer cells. We also report a preliminary assessment of the in vivo pharmacology of [^{18}F]FHBG in a nonhuman primate model.

MATERIALS AND METHODS

Reagents

Kryptofix 2.2.2., potassium carbonate, and solvents were purchased from Aldrich Chemical Co. (Milwaukee, WI). *Limulus* amebocyte lysate (LAL) reagent and *Escherichia coli* endotoxin type 055:B5 were obtained from Endosafe Co. (Charleston, SC). Thioglycollate media and trypticase media were purchased from Becton Dickinson (Cockeysville, MD).

Radiotracer

Sterile, pyrogen-free [^{18}F]FHBG was synthesized following the method developed in our laboratory (*26*). The product was isolated by high-performance liquid chromatography (HPLC) using 15% acetonitrile in water. After isolation, solvent was evaporated, and the product was reconstituted with saline solution. The final product was passed through a 0.22-μm Millipore filter (Millipore, Bedford, MA) and collected into a sterile apyrogenic vial. Sterility and pyrogenicity tests were performed on the final preparations after the radioactivity had decayed. Pyrogenicity was tested using LAL reagent and *E. coli* endotoxin type 055:B5. Sterility was tested using thioglycollate and trypticase media.

Cell Line and Transduction

HT-29 human colon cancer cells were obtained from the American Type Culture Collection (Rockville, MD). Cells were transduced with the retroviral vector G1Tk1SvNa following a literature method (*36*). The construction of the retroviral vector G1Tk1SvNa was described elsewhere (*37*). Briefly, the HSV-tk was inserted into the backbone of pG1XSvNa vector (Gene Therapy Inc., Los Angeles, CA) and was under the control of viral long terminal repeat promoter. The amphotropic packaging cell line PA317 was used to make the viral supernatant, and viral titering was done in NIH3T3 cells (*36*). The HT-29 cells were grown in 100-mm dishes (1×10^7 cells per dish) in the presence of Dulbecco's modified Eagle's medium (DMEM) with a high glucose concentration (4.5 g/L) and supplemented with 2 mmol/L glutamine and 10% fetal bovine serum ([FBS] HyClone Laboratory, Logan, UT). Cells were transduced with the viral supernatants supplemented with 8 μg/mL (1,5-dimethyl-1,5-diazaundecamethylene)polymethobromide (Polybrene; Sigma, St. Louis, MO) at a multiplicity of infection of 1 viral particle per cell. Cells were selected with 0.6 mg/mL G-418 (Geneticin; GIBCO Life Technology, Grand Island, NY) for 10 d and used for RNA extraction. The transduced HT-29 cells displayed >99% transduction by methylene blue staining after selection. Cells in culture were reselected monthly (every 4 or 5 passages) to maintain >99% transduction for experimental work. Cells stored at −80°C in liquid nitrogen maintain >99% transduction indefinitely. The expression of proviral transcript was analyzed by northern hybridization with thymidine kinase probe as well as neomycin complementary DNA probe to verify the expression of the genes. In vivo gene expression in this HT-29 tumor line has been verified by immunocytochemical staining using a polyclonal rabbit antibody against the HSV-tk protein (*36*) and, therefore, was not assayed directly in the tumors grown in this study. The doubling time for transduced cells was 48 h, whereas that for wild-type cells was 24 h.

In Vitro Studies

Transduced and nontransduced control cells (approximately 5 million) were plated in triplicate to a Petri dish (100 mm) and cultured in 10 mL media for 24 h. Logarithmically growing cells were incubated with fresh media (7 mL) and 370 kBq [^{18}F]FHBG for 1 and 5 h. After incubation and removal of media, the cells were washed with phosphate-buffered saline ([PBS] 3 × 10 mL) and exposed to trypsin. After neutralization with 10% FBS in DMEM, cells were centrifuged for 5 min at 1,200 rpm and supernatants were discarded. Cells were resuspended in PBS (4 mL), and the number of viable cells was counted using a hemocytometer. The cell suspensions were further centrifuged and the cell pellets were separated. Cellular radioactivity was measured in a Cobra II Auto Gamma Counter (Packard Instrument Co., Meriden, CT). The ratio of activity uptake in transduced and nontransduced cells was obtained for each of 3 experiments per time point.

To determine the molecular distribution of radiolabel, cells incubated for 5 h with radiotracer were treated with 1N perchloric acid ([PCA] 100 μL per cell pellet), and the acidic mixtures were cooled to 4°C for 10 min. The acidic cell suspensions were combined and centrifuged for 1 min at 14,000 rpm. The supernatant was separated, neutralized with 2.5N KOH, and analyzed by HPLC after removing the perchlorate salt by centrifugation. HPLC was performed using a Waters Associates system (Milford, MA) equipped with model 510 pumps, a variable-wavelength ultraviolet (UV) detector operated at 254 nm, and a C_{18} reversed-phase analytic column (Rainin, Walnut Creek, CA). Elution was performed at a flow of 1 mL/min with a gradient from 95% A (1% acetonitrile [MeCN], 1.5 mmol/L tetrabutylammonium hydroxide, and 1 mmol/L potassium dihydrogen phosphate in water, pH 3.3) and 5% B (30% MeCN, 1.5 mmol/L tetrabutylammonium hydrox-

ide, and 25 mmol/L potassium dihydrogen phosphate in water, pH 3.3) to 50% A and 50% B over a 10-min period, followed by a gradient to 0% A and 100% B over an additional 3 min. Fractions were collected at 30-s intervals using a fraction collector (LKB Pharmacia, Uppsala, Sweden). Radioactivity in each fraction was measured in a γ-counter and plotted.

In Vivo Studies on Mice

In vivo studies, including blood clearance and biodistribution, were conducted on tumor-bearing nude mice at 2 and 5 h after injection. Tumors were grown in 6-wk-old athymic nude mice (Harlan–Sprague–Dawley; Harlan, Indianapolis, IN) by inoculation of 10 million cells (either transduced or nontransduced) under the skin in the left thigh region. When the tumor was approximately 1 cm in size, animals were used for the experiment as described below. Animal studies were performed under an approved institutional animal care and use committee (IACUC) protocol.

Four groups of mice ($n = 5$ per group), 2 with transduced tumors and 2 with nontransduced tumors, were injected intravenously through a tail vein with the radiotracer [^{18}F]FHBG (approximately 2 MBq; 200 μL). Activity injected into each mouse was measured by placing the mouse in a dose calibrator (Capintec, Ramsey, NJ). In 3 randomly selected mice bearing transduced tumors, blood was collected in capillary tubes (1.33 μL) from the contralateral tail vein after rupture with a needle; samples were obtained 1, 2, 5, 10, 20, 40, 60, and 120 min after injection. Activity in each blood sample was measured with the γ-counter, and the percentage injected dose per gram of body weight (%ID/g) was calculated. Animals were anesthetized with sodium pentobarbital (40 mg/kg) and sacrificed at 2 or 5 h after injection. Organs and tumors were excised and weighed. Tissue radioactivity was measured with the γ-counter. For each mouse, [^{18}F]FHBG uptake was expressed as the %ID/g and as the ratio of tumor to organ uptake.

In Vivo Studies on Monkeys

Two male cynomolgus monkeys (5.2 and 7.0 kg) (*Macaca fascicularis*; Biomedical Resources Foundation, Inc., Houston, TX) were anesthetized with sodium pentobarbital and prepared for arterial blood sampling by catheterization of a femoral artery. The animals were positioned supine in a CTI/Siemens 953A PET scanner (Knoxville, TN) and injected intravenously with 23–28 MBq/kg [^{18}F]FHBG. Five sequential whole-body, attenuation-corrected PET scans of increasing duration were obtained between 0 and 2 h after injection. Blood samples were taken at increasing intervals from 30 s to 120 min after injection. A urine sample was also obtained from 1 monkey by transabdominal puncture. Blood samples were immediately placed in ice and then centrifuged. An aliquot was removed from each sample, weighed, and counted for radioactivity. In samples drawn for metabolite analysis, the remaining plasma was prepared for HPLC analysis by acid extraction with PCA (1N), and neutralization with KOH (4 mol/L). The acid-soluble fraction (ASF) was analyzed by ion-pair HPLC using a C_8 reversed-phase analytic column (Radial Pak; Waters) and isocratic elution. The mobile phase consisted of 5% MeCN in 20 mmol/L phosphate buffer containing 2.5 mmol/L tetrabutylammonium hydroxide (pH 6.5), and the flow was 1.0 mL/min. Eluents were passed through an in-line UV detector (Waters), and eluted fractions were collected and assayed for radioactivity. Metabolites and [^{18}F]FHBG eluted within 12 min. The procedure for analysis of the molecular distribution of radiolabel in urine was the same as that for plasma. Monkeys were studied under an approved IACUC protocol.

RESULTS

Radiotracer Synthesis

The [^{18}F]FHBG was prepared in 10%–15% yield (*26*). All preparations showed the radiochemical purity of [^{18}F]FHBG to be >99%. Specific activity ranged from 15 to 26 GBq/μmol. All preparations used in these studies were found to be sterile and apyrogenic.

Uptake and Biodistribution Studies

Figure 1 summarizes uptake of [^{18}F]FHBG in vitro in transduced and nontransduced cells. At 1 and 5 h, activity uptake in transduced cells was 31 ($P < 0.001$) and 71 ($P < 0.001$) times higher, respectively, than that in the control cells. Figure 2 shows HPLC radiochromatograms of the ASF from transduced and nontransduced cells at 5 h of incubation. Four radioactive peaks were observed for transduced cells, corresponding to the parent compound and its presumed mono-, di-, and triphosphates, estimated as 10%, 6%, 54%, and 30% of recovered activity, respectively. The peak at 11 min is attributed to [^{18}F]FHBG, whereas the peaks at 16, 20.5, and 23.5 min were tentatively assigned as mono-, di-, and triphosphates, respectively. Analysis of the ASF of nontransduced cells showed only 1 radioactive peak at 11 min, which corresponds to the parent compound [^{18}F]FHBG.

The blood clearance curve for [^{18}F]FHBG in nude mice, uncorrected for metabolites, is shown in Figure 3. Radioactivity cleared rapidly from the blood. The peak radioactivity was seen at 2 min after tail vein injection, after which a biphasic decrease was observed. The slower phase (20–120 min) had a half-time of about 40 min.

Tables 1 and 2 summarize the biodistribution of [^{18}F]FHBG in tumor-bearing nude mice at 2 and 5 h after

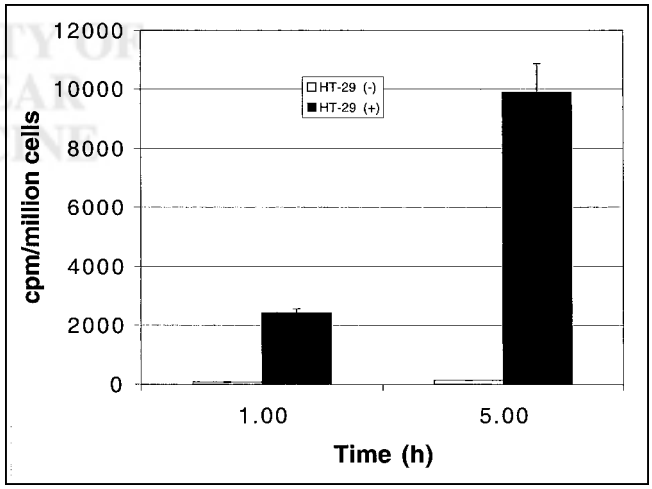

FIGURE 1. In vitro incorporation of [^{18}F]FHBG into transduced (+) and nontransduced (−) cells at 1 and 5 h. Data are average of 3 experiments ± SEM; $P < 0.001$ for both time points (Student t test). cpm = counts per minute.

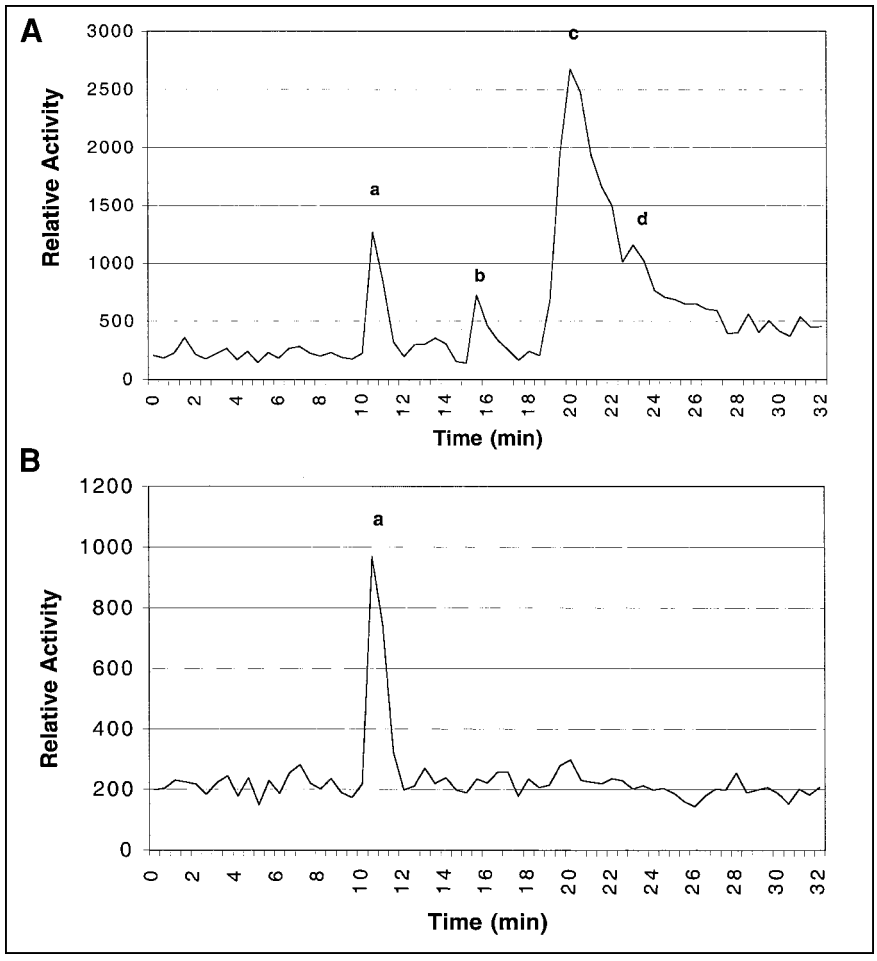

FIGURE 2. HPLC radiochromatograms of [^{18}F]FHBG (a) and its metabolites (b–d) in HT-29 tumor cells after 5-h incubation. (A) Transduced cells. (B) Nontransduced cells.

injection, respectively. At 2 h, activity uptake in transduced tumors was 4-fold higher than that in the control tumors. Bone uptake was relatively high compared with that in other organs. At 5 h, activity uptake in transduced tumors was approximately 13-fold higher than that in the control tumors. Bone uptake compared with that in other organs at this time point was higher than that at 2 h. Absolute uptake in transduced tumors decreased somewhat between 2 and 5 h. Activity concentration in transduced tumors was ≥5 times that in normal tissues and organs other than bone at 2 and 5 h.

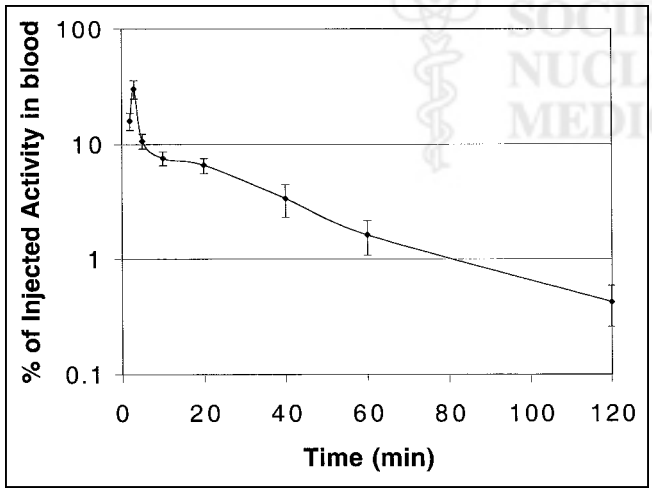

FIGURE 3. Blood clearance curve of ^{18}F activity in nude mice bearing transduced tumors after intravenous injection of [^{18}F]-FHBG (semilogarithmic plot; $n = 3$).

A plasma time–activity concentration curve for ^{18}F in monkeys is shown in Figure 4. As in mice, the clearance of radioactivity was very rapid, with an estimated 1% and 0.1% of injected activity remaining in plasma at 5 and 120 min, respectively. Figure 5 shows a representative HPLC radiochromatogram of a plasma sample from a monkey at 60 min after injection. Data for the molecular distribution of radiolabel in plasma and urine versus time are summarized in Table 3. Unidentified radiolabeled metabolite(s) of [^{18}F]FHBG was present in measurable amounts by 15 min and increased progressively to about 30% of total activity in plasma by 2 h. Almost all ^{18}F in urine at 2 h after injection was present as [^{18}F]FHBG. Images from 1 PET study of a monkey injected with [^{18}F]FHBG are shown in Figure 6.

DISCUSSION

The goal of this work was to develop an effective radiotracer for imaging gene incorporation and expression in

TABLE 1
Biodistribution of [^{18}F]FHBG in Tumor-Bearing Mice at 2 Hours

Tissue	Nontransduced tumor model		Transduced tumor model	
	%ID/g	Tumor-to-tissue ratio	%ID/g	Tumor-to-tissue ratio
Blood	0.035 ± 0.003	3.37 ± 0.11	0.041 ± 0.002	12.12 ± 0.91
Skin	0.056 ± 0.004	2.09 ± 0.12	0.046 ± 0.004	17.12 ± 4.25
Muscle	0.034 ± 0.002	3.49 ± 0.22	0.039 ± 0.005	21.93 ± 4.09
Bone	0.243 ± 0.013	0.53 ± 0.06	0.258 ± 0.024	2.46 ± 0.33
Heart	0.037 ± 0.003	3.24 ± 0.18	0.033 ± 0.005	24.93 ± 3.75
Lung	0.055 ± 0.005	2.14 ± 0.08	0.052 ± 0.004	12.59 ± 2.29
Liver	0.007 ± 0.014	1.65 ± 0.32	0.119 ± 0.016	6.29 ± 0.89
Spleen	0.074 ± 0.006	1.62 ± 0.11	0.068 ± 0.006	10.35 ± 2.08
Pancreas	0.073 ± 0.006	1.79 ± 0.18	0.074 ± 0.006	7.96 ± 1.14
Stomach	0.062 ± 0.009	2.45 ± 0.27	0.075 ± 0.030	8.27 ± 1.23
Intestine	0.099 ± 0.008	1.47 ± 0.23	0.110 ± 0.005	4.74 ± 0.43
Kidney	0.129 ± 0.007	0.98 ± 0.12	0.116 ± 0.012	5.48 ± 0.67
Tumor	0.113 ± 0.008		0.508 ± 0.049*	

*$P < 0.05$ compared with nontransduced tumor (Student *t* test on paired samples).
Data are mean ± SEM of 5 animals.

transduced tumor cells using PET. The penciclovir derivative [^{18}F]FHBG was prepared in sterile, pyrogen-free form in amounts (555–740 MBq) suitable for in vitro cellular and in vivo animal and human studies. Our results support the hypothesis that this agent is a substrate for HSV-tk and has advantages for imaging compared with a similar analog of ganciclovir labeled with ^{18}F—namely, FHPG.

In vitro studies revealed a much higher accumulation of [^{18}F]FHBG with time in transduced cells compared with that in nontransduced control cells, consistent with monophosphorylation of the tracer by HSV-tk. Similar patterns of accumulation of [^{3}H]ganciclovir and [^{18}F]FHPG have been observed in virus-infected and transduced cells (*2,28*). However, uptake of [^{18}F]FHBG at 5 h was 12-fold higher than that of [^{18}F]FHPG in the same cell line (*28*), suggesting that the rate of phosphorylation of [^{18}F]FHBG by HSV-tk or stability (or both) and intracellular retention of nucleotides thus formed is much higher than that with [^{18}F]FHPG. A similar relationship has been shown for the parent compounds penciclovir and ganciclovir in virus-infected cell lines (*5,7,12*).

In control cells, no significant uptake of [^{18}F]FHBG was observed over time, with the small amount of activity uptake representing nonspecific accumulation of the parent compound. That cellular accumulation of FHBG is unrelated to cell growth is supported by the observed 2-fold higher cell growth rate in wild-type cells (doubling time, 24 h) compared with that in transduced cells (dou-

TABLE 2
Biodistribution of [^{18}F]FHBG in Tumor-Bearing Mice at 5 Hours

Tissue	Nontransduced tumor model		Transduced tumor model	
	%ID/g	Tumor-to-tissue ratio	%ID/g	Tumor-to-tissue ratio
Blood	0.017 ± 0.001	1.58 ± 0.14	0.017 ± 0.001	20.71 ± 1.06
Skin	0.026 ± 0.001	1.05 ± 0.07	0.030 ± 0.001	11.52 ± 0.62
Muscle	0.017 ± 0.001	1.64 ± 0.12	0.022 ± 0.003	22.23 ± 2.41
Bone	0.225 ± 0.015	0.13 ± 0.01	0.220 ± 0.015	1.71 ± 0.15
Heart	0.020 ± 0.001	1.48 ± 0.15	0.023 ± 0.001	15.74 ± 0.99
Lung	0.031 ± 0.002	0.89 ± 0.06	0.022 ± 0.001	15.73 ± 0.93
Liver	0.047 ± 0.002	0.54 ± 0.02	0.034 ± 0.002	11.23 ± 1.01
Spleen	0.050 ± 0.003	0.55 ± 0.04	0.043 ± 0.003	9.08 ± 0.99
Pancreas	0.028 ± 0.003	1.46 ± 0.28	0.029 ± 0.001	11.49 ± 0.51
Stomach	0.050 ± 0.003	0.84 ± 0.08	0.030 ± 0.001	11.51 ± 0.68
Intestine	0.064 ± 0.005	0.47 ± 0.05	0.058 ± 0.002	5.87 ± 0.27
Kidney	0.054 ± 0.002	0.49 ± 0.03	0.048 ± 0.005	8.86 ± 1.11
Tumor	0.025 ± 0.010		0.335 ± 0.070*	

*$P < 0.001$ compared with nontransduced tumor (Student *t* test on paired samples).
Data are mean ± SEM of 5 animals.

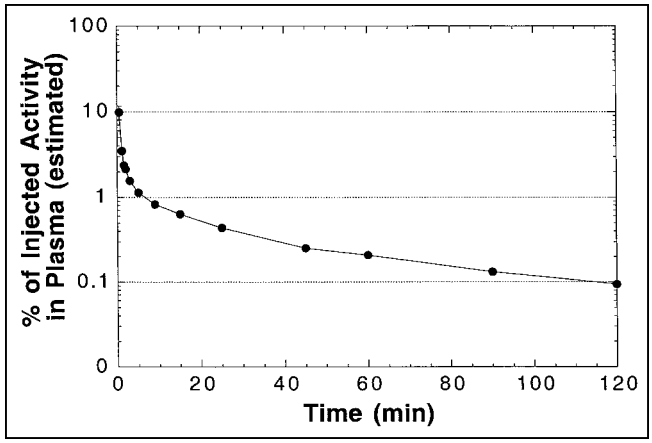

FIGURE 4. Time–activity curve for arterial plasma from cynomolgus monkeys after intravenous injection of [18F]FHBG (semilogarithmic plot). Total plasma volume was estimated to be 2.5% of body weight in calculating %ID in plasma. Data are mean ± SEM from 2 monkeys. Error bars are smaller than symbols for most data points. Solid line is intended to guide the eye and does not represent model fit to data.

bling time, 48 h). Thus, higher uptake in transduced cells supports the hypothesis that the tracer is selectively phosphorylated by HSV-tk only and not by native thymidine kinase.

HPLC analysis of the ASF of the transduced cells after 5 h of incubation with [18F]FHBG showed 4 radioactive peaks. The elution profile of these peaks is consistent with that of [3H]penciclovir and its phosphates in cultured cells (*12*). In the analysis of a mixture of standard guanosine and its phosphates, the nucleoside and mono-, di-, and triphosphates had similar retention times of 10.5, 15.5, 19.7, and 22.8 min in our HPLC system. By analogy, the second peak in the experiments with [18F]FHBG has been assigned as the monophosphate, the third peak as the diphosphate, and the fourth peak as the triphosphate of [18F]FHBG. The intensity of the triphosphate peak was less compared with that of the diphosphate. Because nucleoside triphosphates are known to be relatively unstable (*38*), some of the triphosphate may have been hydrolyzed to the more stable diphosphate during the work-up, leading to inaccuracies regarding the relative proportions observed by HPLC. Because standard unlabeled phosphates of FHBG are not available, assignment of these nucleotides is tentative, and further studies on gradient elution for separation and identification of these phosphates are necessary for precise identification of these species. However, presumptive identification of these species suggests that, after monophosphorylation by HSV-tk, FHBG, like its parent compound penciclovir, is converted into its di- and triphosphates.

In vivo blood clearance studies showed that radioactivity from injected [18F]FHBG was cleared rapidly and monotonically in mice and monkeys. This agrees with observations of [18F]FHPG in nude mice (*28*) and [18F]-

TABLE 3
Distribution of Radiolabel from [18F]FHBG Among Acid-Soluble Molecules in Plasma and Urine of Cynomolgus Monkeys

Tissue	Time after injection (min)	Recovered activity on FHBG*† (%)
Plasma	0	99.5 ± 0.2 (2)
Plasma	15	91 ± 1 (2)
Plasma	60	87 ± 1 (2)
Plasma	120	69 ± 6 (2)
Urine	120	97 (1)

*Data are mean ± SEM (no. of observations).
†Measured recovery of radioactivity from HPLC was 89% ± 2% (mean ± SEM), which was determined according to method described in legend to Figure 5.

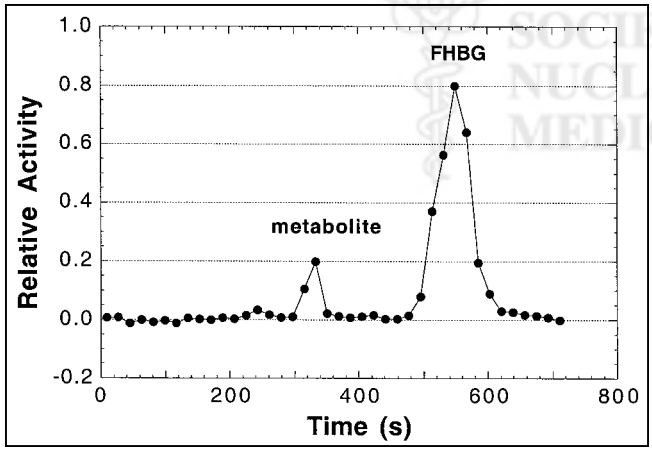

FIGURE 5. HPLC radiochromatogram of [18F]FHBG and its metabolites in plasma taken 60 min after injection from cynomolgus monkey. For study shown, 86% of recovered activity was on [18F]FHBG as calculated by FHBG peak area ÷ total area under radiochromatogram.

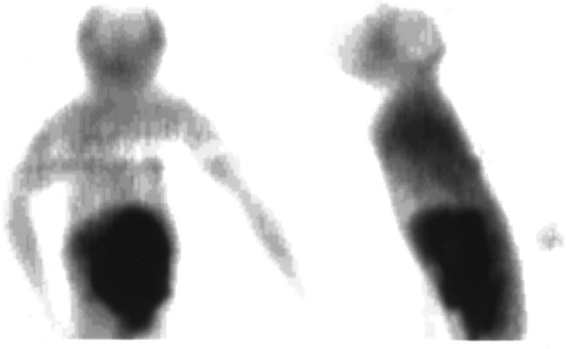

FIGURE 6. Distribution of 18F from [18F]FHBG in cynomolgus monkey. Images are coronal (left) and sagittal (right) 2-dimensional projections from multicouch-position scan obtained 104–140 min after intravenous injection of [18F]FHBG. Note that skeleton is not visualized, indicating that 18F uptake in bone and marrow was relatively low.

FHBG in healthy human volunteers (*39*). At 2 h after injection in nude mice, uptake of [^{18}F]FHBG was greater than that seen previously with [^{18}F]FHPG for most organs and tissues studied (Fig. 7A). ^{18}F from the 2 radiotracers washed out of most normal tissues and organs at approximately the same fractional rates between 2 and 5 h (Fig. 7). The one exception was bone. Earlier in vivo studies with [^{18}F]FHPG in nude mice did not show uptake in bone matrix—that is, nearly all activity within bone samples was accounted for in the marrow and washed out with time (*28*). However, in the case of [^{18}F]FHBG, activity concentration within bone samples was almost as high at 5 h as at 2 h, indicating that the activity did not wash out with time. Bone uptake could be attributed to the accumulation of the radiotracer in bone marrow or free fluoride in bone (or both). To differentiate between bone and marrow uptake, bones were treated with 0.5% sodium dodecyl sulfate, and marrow was removed using a needle. Bones without marrow were counted again, and no significant change of activity was observed after removal of marrow. At 5 h, 92% ± 3% of the activity was in the bone matrix compared with 89% ± 4% at 2 h. These results support the hypothesis that activity in bone at both times was predominately caused by incorporation of free fluoride by the bone matrix in addition to some nonspecific tracer uptake in the marrow. The close similarity of mean bone uptake among the 4 groups of mice (control and transduced tumors at 2 and 5 h) and the relatively small SDs for bone uptake indicate that the degree of defluorination was similar among individual mice. Finally, as shown in Figure 6, the high uptake of ^{18}F in bone detected in mice did not occur in monkeys. Thus, there appears to be a significant difference between mice and monkeys with regard to defluorination of FHBG. As in the cell studies discussed above, higher in vivo uptake in transduced tumors compared with nontransduced tumors supports the hypothesis that [^{18}F]FHBG is selectively phosphorylated by HSV-tk. By 5 h, the tumor-to-blood ratio in transduced tumors was approximately 21, whereas for nontransduced tumors it remained low, at approximately 1.6 (Table 2). The %ID/g in transduced tumors was approximately 13-fold higher

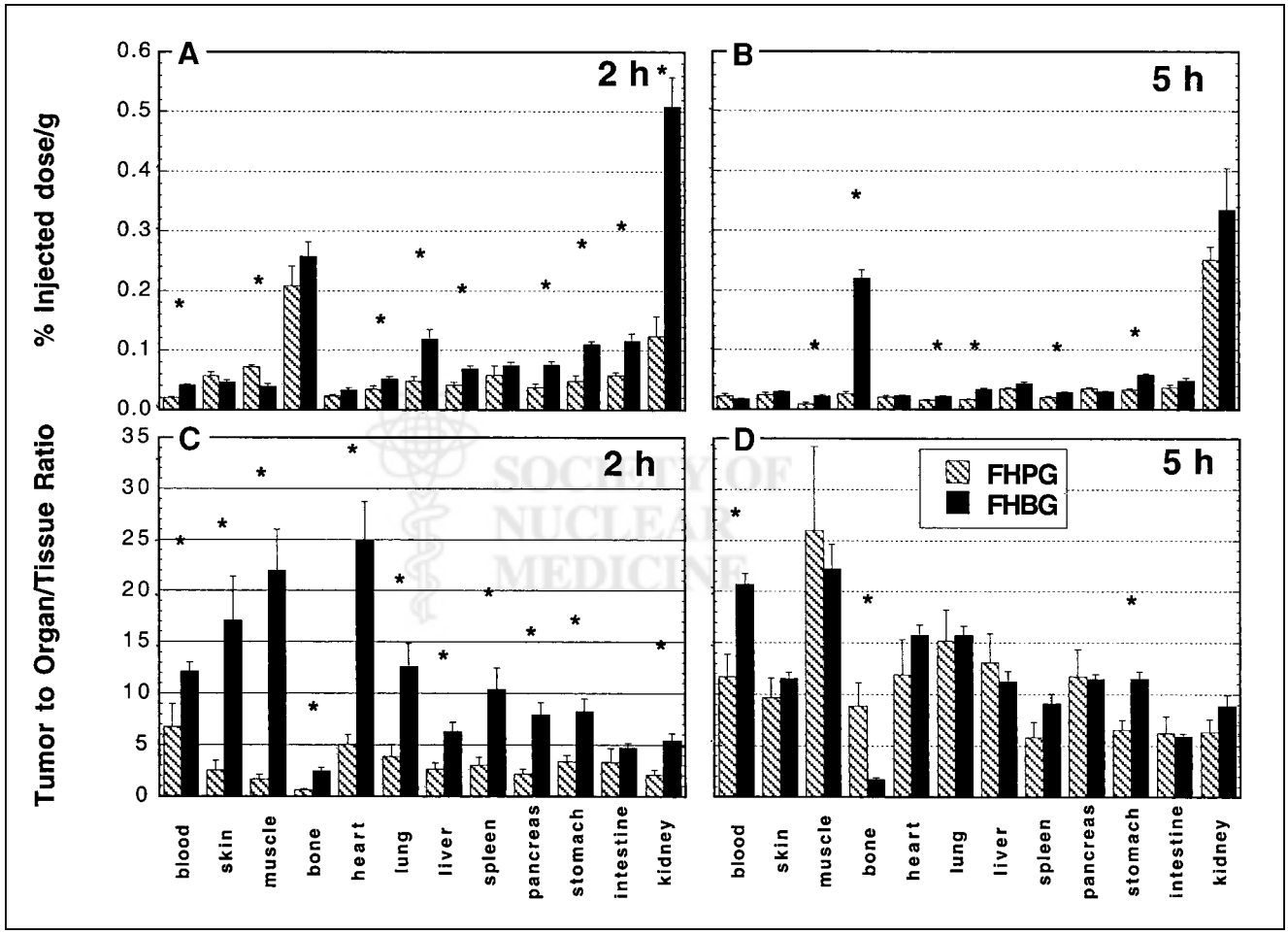

FIGURE 7. Biodistribution of radiolabel from [^{18}F]FHBG and [^{18}F]FHPG in nude mice bearing transduced tumors. (A) Uptake at 2 h after injection. (B) Uptake at 5 h after injection. (C) Tumor-to-normal ratios at 2 h after injection. (D) Tumor-to-normal ratios at 5 h after injection. Data are mean ± SEM (n = 5). *$P < 0.05$ for difference between FHPG and FHBG.

than that in the nontransduced tumors at this time point. This finding is likely related to washout of nonspecifically bound drug and clearance of the background activity along with continued trapping of the remaining circulating parent compound, which presumably accounts for the increasing retention of drug in transduced cells over time.

The results in mice suggest that an enhancement of image quality will be achieved with [^{18}F]FHBG compared with that of [^{18}F]FHPG, at least during the first 2 h after injection. At 2 h, uptake in transduced tumors was 4-fold greater with [^{18}F]FHBG than that with [^{18}F]FHPG (Fig. 7A), and transduced tumor-to-normal tissue ratios were much greater for [^{18}F]FHBG than those for [^{18}F]FHPG (Fig. 7C). However, transduced tumors continued to accumulate radiolabel from [^{18}F]FHPG between 2 and 5 h, whereas there was a decline in tumor uptake during this time period for [^{18}F]FHBG (Fig. 7B). Because of this finding, the relative advantage of [^{18}F]FHBG with regard to tumor-to-normal contrast is lost by 5 h (Fig. 7D). The observed decline in absolute tumor uptake between 2 and 5 h with [^{18}F]FHBG presumably reflects washout of nonphosphorylated radiolabel, including perhaps ^{18}F fluoride, in parallel with declining blood levels of ^{18}F. More detailed kinetic studies are required to address the long-term kinetic behavior of [^{18}F]FHBG relative to that of [^{18}F]FHPG.

Direct assay of circulating metabolites of [^{18}F]FHBG was not done in mice but was addressed in the nonhuman primate model. When coupled with the rapid disappearance of radiolabel from the blood (Fig. 5), the data indicate that the contribution of labeled metabolites to integral plasma activity remains small during the first 2 h after injection of [^{18}F]FHBG (Table 3). This finding implies that the exposure of tumors and normal tissues to circulating metabolites of the injected compound is small, as reflected in the observation that 97% of the activity seen in urine at 2 h was on [^{18}F]FHBG. Similar results were reported for the urine of normal human volunteers at 2 h, although the presence of plasma metabolites was not addressed (*39*).

CONCLUSION

In vitro and in vivo studies indicate that [^{18}F]FHBG is selectively phosphorylated by the HSV-tk enzyme and show a high ratio of uptake in transduced tumor cells compared with nontransduced tumor cells as well as normal tissues and organs. In comparison with [^{18}F]FHPG, [^{18}F]FHBG provides much higher tumor-to-normal tissue ratios at 2 h after injection. Bone uptake of ^{18}F in mice is higher for FHBG than for FHPG, presumably because of partial in vivo defluorination. However, defluorination and recirculating, labeled metabolites of [^{18}F]FHBG are minor effects in monkeys, suggesting that they would not be serious impediments to the usefulness of the radiotracer in humans. In summary, these observations indicate that [^{18}F]FHBG may yield high-contrast PET images of HSV-tk expression in tumors and, therefore, show promise for use in conjunction with suicide gene therapy of cancer.

REFERENCES

1. Boyd MR, Bacon TH, Sutton D, Cole M. Antiherpes virus activity of 9-(4-hydroxy-3-hydroxymethylbut-1-yl)guanine (BRL 39123) in cell culture. *Antimicrob Agents Chemother.* 1987;31:1238–1242.
2. Cheng Y-C, Grill SP, Dutschman GE, Nakayama K, Bastow KF. Metabolism of 9-(1,3-dihydroxy-2-propoxymethyl)guanine, a new anti-herpes virus compound in herpes simplex virus-infected cells. *J Biol Chem.* 1983;258:12460–12464.
3. Elion GB, Furman PA, Fyfe JA, De Miranda P, Beauchamp L, Schaeffer HJ. Selectivity of action of an antiherpetic agent, 9-(2-hydroxyethoxymethyl)guanine. *Proc Natl Acad Sci USA.* 1977;74:5716–5720.
4. Martin JC, Dvorak CA, Smee DF, Matthews TR, Verheyden JPH. 9-[(1,3-Dihydroxy-2-propoxy)methyl]guanine: a new selective antiherpes agent. *J Med Chem.* 1983;26:759–771.
5. Smee DF, Boehme R, Chernow M, et al. Intracellular metabolism and enzymatic phosphorylation of 9-(1,3-dihydroxy-2-propoxymethyl)guanine and acyclovir in herpes simplex virus infected and uninfected cells. *Biochem Pharmacol.* 1985; 34:1049–1056.
6. Smee DF, Martin JC, Verheyden JPH, Binko BP, Matthews TR. Anti-herpes virus activity of the acyclic nucleoside 9-(1,3-dihydroxy-2-propoxymethyl)guanine. *Antimicrob Agents Chemother.* 1983;23:676–682.
7. Boyd MR, Bacon TH, Sutton D. Antiherpes virus activity of 9-(4-hydroxy-3-hydroxymethylbut-1-yl)guanine (BRL 39123) in animals. *Antimicrob Agents Chemother.* 1988;32:358–363.
8. Earnshaw DL, Bacon TH, Darlison SJ, Edmonds K, Perkins RM, Vere Hodge RA. Mode of antiviral action of penciclovir in MRC-5 cells infected with herpes simplex virus type 1 (HSV-1), HSV-2, and varicella-zoster virus. *Antimicrob Agents Chemother.* 1992;36:2747–2757.
9. Martin JC, McGee D, Jeffrey G, et al. Synthesis and anti-herpes-virus activity of acyclic 2′-deoxyguanosine analogues related to 9-[(1,3-dihydroxy-2-propoxy)-methyl]-guanine. *J Med Chem.* 1986;29:1384–1389.
10. Schaeffer HJ, Bauchamp L, De Miranda P, Elion G. 9-(2-Hydroxyethyloxy-methyl)-guanine activity against viruses of the herpes group. *Nature.* 1978;272: 583–585.
11. Smee DF, Campbell NL, Matthews TR. Comparative anti-herpes-virus activities of the 9-(1,3-dihydroxy-2-propoxymethyl)guanine, acyclovir, and two 2′-fluoro-pyrimidine nucleosides. *Antiviral Res.* 1985;5:259–267.
12. Vere Hodge RA, Perkins RM. Mode of action of 9-(4-hydroxy-3-hydroxymethyl-but-1-yl)guanine (BRL 39123) against herpes simplex virus in MRC-5 cells. *Antimicrob Agents Chemother.* 1989;33:223–229.
13. Culver KW, Ram Z, Wallbridge S, Ishi H, Oldfield EH, Blaese RM. *In vivo* gene transfer with retroviral vector-producer cells for treatment of experimental brain tumors. *Science.* 1992;256:1550–1552.
14. Oldfield EH, Ram Z, Culver K, et al. Clinical protocols: gene therapy for the treatment of brain tumors using intra-tumoral transduction with the thymidine kinase gene and intravenous ganciclovir. *Hum Gene Ther.* 1993;4:39–69.
15. Ram Z, Culver KW, Wallbridge S, Blaese RM, DeVroom HL, Anderson W. In situ retroviral-mediated gene transfer for the treatment of brain tumors in rats. *Cancer Res.* 1993;53:83–88.
16. Culver KW, Blaese RM. Gene therapy for cancer. *Trends Genet.* 1994;10:174–178.
17. Huber BE, Richard CA, Krenitski TA. Retroviral mediated gene therapy for the treatment of hepatocellular carcinoma: an innovative approach for cancer therapy. *Proc Natl Acad Sci USA.* 1991;88:8039–8043.
18. Vile RG, Hart IR. Use of tissue specific expression of the herpes simplex virus thymidine gene to inhibit growth of established murine melanomas following direct intramural injection of DNA. *Cancer Res.* 1993;53:3860–3864.
19. Haberkorn U, Oberdorfer F, Gebert J, et al. Monitoring of gene therapy with cytosine deaminase: in vitro studies using ^{3}H-5-fluorocytosine. *J Nucl Med.* 1996;37:87–94.
20. Haberkorn U, Altmann A, Morr I, Germann C, Oberdorfer F, Van Kaick G. Multitracer studies during gene therapy of hepatoma cells with herpes simplex virus thymidine kinase and ganciclovir. *J Nucl Med.* 1997;38:1048–1054.
21. Haberkorn U, Altmann A, Morr I, et al. Monitoring gene therapy with herpes simplex virus thymidine kinase in hepatoma cells: uptake of specific substrates. *J Nucl Med.* 1997;38:287–294.
22. Conti PS, Lilien DL, Grafton ST, Bading JR, Keppler J, Hawley K. PET and [^{18}F]-FDG in oncology: a clinical update. *Nucl Med Biol.* 1996;23:717–735.
23. Tjuvajev JG, Stockhammar G, Desai R, et al. Imaging the expression of transfected genes *in vivo*. *Cancer Res.* 1995;55:6126–6132.

24. Alauddin MM, Conti PS, Mazza SM, Hamzeh FM, Lever JR. Synthesis of 9-[(3-[^{18}F]fluoro-1-hydroxy-2-propoxy)methyl]guanine ([^{18}F]FHPG): a potential imaging agent of viral infection and gene therapy using PET. *Nucl Med Biol.* 1996;23:787–792.
25. Bading JR, Alauddin MM, Fissekis JD, Kirkman E, Raman RK, Conti PS. Pharmacokinetics of F-18 fluorohydroxy-propoxymethyl-guanine (FHPG) in primates [abstract]. *J Nucl Med.* 1997;39(suppl):43P.
26. Alauddin MM, Conti PS. Synthesis and preliminary evaluation of 9-(4-[^{18}F]-fluoro-3-hydroxymethylbutyl)guanine ([^{18}F]-FHBG): a new potential imaging agent for viral infection and gene therapy using PET. *Nucl Med Biol.* 1998;25: 175–180.
27. Gambhir SS, Barrio JR, Wu L, et al. Imaging of adenoviral-directed herpes simplex virus type 1 thymidine kinase reporter gene expression in mice with radiolabeled ganciclovir. *J Nucl Med.* 1998;39:2003–2011.
28. Alauddin MM, Kundu R, Gordon EM, Conti PS. Evaluation of 9-(3-[^{18}F]-fluoro-1-hydroxy-2-propoxymethyl)guanine ([^{18}F]-FHPG) *in vitro* and *in vivo* as a probe for PET imaging of gene incorporation and expression in tumors. *Nucl Med Biol.* 1999;26:371–376.
29. deVaries EFJ, Hospers GAP, Doze P, van Waarde A, Mulder NH, Waalburg W. PET imaging of HSV thymidine kinase activity with 9-(3-[^{18}F]-fluoro-1-hydroxy-2-propoxymethyl)guanine ([^{18}F]-FHPG) [abstract]. *J Labelled Compd Radiopharm.* 1999;42(suppl):S7–S9.
30. Monclus M, Damhaut P, Kuhnast B, et al. *In vivo* validation in rat and monkey of *RAC*-9-(3-[^{18}F]-fluoro-1-hydroxy-2-propoxymethyl)guanine: a radiopharmaceutical for gene therapy [abstract]. *J Labelled Compd Radiopharm.* 1999; 42(suppl):S10–S12.
31. Namavari M, Barrio JR, Toyokuni T, et al. Synthesis of 8-[^{18}F]fluoroguanine derivatives: *in vivo* probes for imaging gene expression with positron emission tomography. *Nucl Med Biol.* 2000;27:157–162.
32. Yaghoubi SS, Nguyen K, Bauer E, et al. Imaging adenoviral mediated therapeutic gene delivery by co-administration of a second adenovirus carrying a PET reporter gene [abstract]. *J Nucl Med.* 2000;41(suppl):37P.
33. Sun X, Barrio JR, Toyokuni T, et al. Quantitation of gene induction by PET imaging of a bi-directional tetracyclin-inducable reporter gene system in living animals [abstract]. *J Nucl Med.* 2000;41(suppl):38P.
34. Green LA, Nguyen K, Berenji B, et al. Tracer kinetic modeling of FHBG in mice imaged with microPET for quantitation of reporter gene expression [abstract]. *J Nucl Med.* 2000;41(suppl):58P.
35. Iyer M, Bauer B, Barrio JR, et al. Comparison of FPCV, FHBG and FIAU as reporter probes for imaging herpes simplex virus type 1 thymidine kinase reporter gene expression [abstract]. *J Nucl Med.* 2000;41(suppl):80P.
36. Yang L, Hwang R, Chiang Y, Gordon EM, Anderson WF, Parekh D. Mechanism for ganciclovir resistance in gastrointestinal tumor cells transduced with retroviral vector containing the herpes simplex virus thymidine kinase gene. *Clin Cancer Res.* 1998;4:731–741.
37. Lyons RM, Forry-Schaudies S, Otto E, et al. An improved retroviral vector encoding the herpes simplex virus thymidine kinase gene increasing antitumor efficacy *in vivo. Cancer Gene Ther.* 1995;2:273–280.
38. Campbell NA. *Biology.* 3rd ed. Redwood City, CA: Benjamin/Cumming Publishing; 1993:98–99.
39. Yaghoubi SS, Goldman R, Barrio JR, et al. PET imaging of FHBG in humans: a tracer for monitoring herpes simplex virus type 1 thymidine kinase suicide gene therapy [abstract]. *J Nucl Med.* 2000;41(suppl):73P.